CHARACTERISTICS OF FLOW OVER PARABOLIC BROAD-CRESTED WEIR

M.A. Abourehim
Irrigation and Hydraulics Department, Faculty of Engineering,
Alexandria University, Alexandria, Egypt.

ABSTRACT

A discharge measurement device using broad-crested weir with parabolic cross section provides wide measuring range without any effect on the head-discharge relationship by tail water up to high submergence ratio. The present work presents theoretical and experimental analyses for the characteristics of flow over such weir. The depth of flow over weir, the velocity coefficient C_v, the discharge coefficient C_d, and the brink depth are analysed theoretically via applying the energy equation. Theoretical relationships were developed. The submergence criterion and the water surface profile are experimentally investigated using weir model of various dimensions. The developed relationships are verified by the experimental measurements, and a good agreement was found to exist. Finally, a head-discharge relationship are presented in terms of mathematical formulas and charts.

NOMENCLATURE

A	Area of the flow cross section,
A_c	Area of critical flow cross section,
b	Channel bed width,
C_d	Discharge coefficient,
C_v	Velocity coefficient,
H	Head on weir crest,
H_o	Total head on weir, $H_o = H + \dfrac{\alpha_1 va^2}{2g}$,
h_s	The submergence head of tail water,
L	Length of weir crest,
P	The parameter of the parabola,
Q	Discharge passing over weir,
S	Initial submergence ratio corresponds to submergence starting effect
T	Top width of flow cross section,
T_c	Top width of critical flow cross section,
v_a	Velocity of the approaching flow,
v_b	Velocity of flow at the brink section
v	Velocity of flow over weir at the contracted section,
y	Depth of flow over weir,
y_b	Depth of flow at the brink section,
y_c	Depth of critical flow, $y_c = \left(\dfrac{27}{64}\cdot\dfrac{Q^2}{g\,P}\right)^{1/4}$
y_f	Depth of free flow over weir,
y_s	Depth of submerged flow over weir,
α_1, α_2	Energy correction coefficients,
η	Coefficient of head loss.

1.INTRODUCTION

The determination of stream discharges has a great importance in the operation efficiency of many projects in; irrigation developments, water supply, river engineering hydrologic studies on experimental basins, and in many other practical situations. It is appropriate therefore, to re-evaluate the existing methods of flow measurement to improve their accuracies, and to develop new methods of better accuracies. Furthermore, the larger the number of methods available, the better is the chance for designers to select the most suitable method to their various applications.

Broad-crested weir referred to as critical depth meters, on which critical depth is assumed to be occurred. The parshall flume, rectangular, trapezoidal and triangular brood-crested weirs, and rectangular cutthroat measuring flume, are examples of flow measuring methods based on this principle [1,2,3,4,5,6,7,8,9,10,11]. Critical depth meter is solely valid for ideal flow in which the loss of flow energy is neglected. The assumption of ideal flow causes an error of about 10% in discharge prediction, [12]. Actually, a part of the approaching flow energy is lost due to the lateral and vertical contractions through such structures, which makes the depth of flow to be less than the critical depth. For various dimensions of rectangular broad-crested weir, its found that the average values of flow depth over weir are 0.524 H and 0.485 H according to Minneseta, and Washington tests, respectively [13]. Also, the 0.524 H value is confirmed experimentally, and theoretically, while the critical depth was found equal to $0.67\ (C_v)^{4/3}$ H [14], where, H is the head on the weir, and C_v is the velocity coefficient.

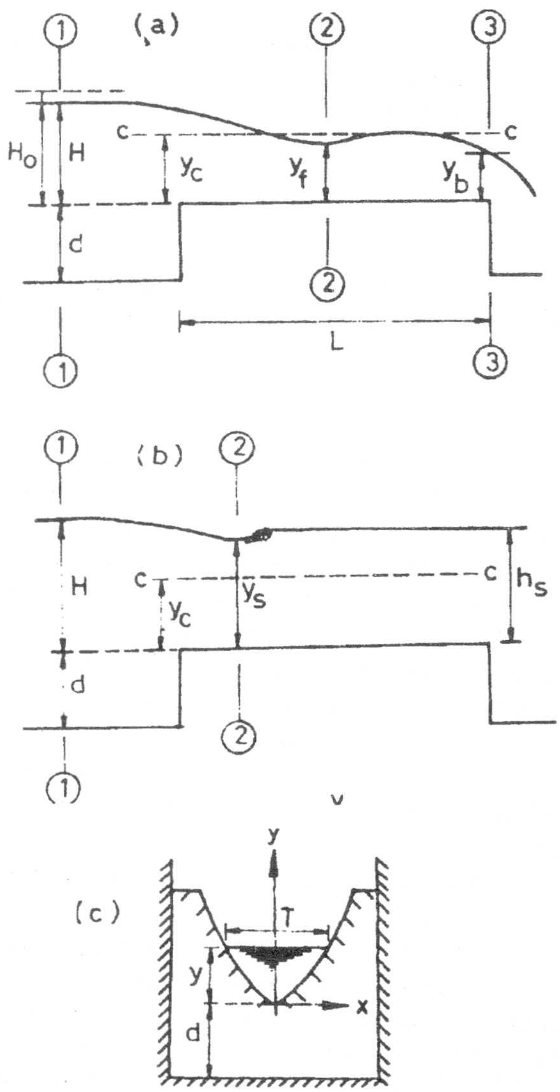

Figure 1. Flow over parabolic broad crested weir, (a) free flow condition, (b) submerged flow condition, (c) cross section.

Consequently, for accurate discharge measurements the discharge equations should be based on the actual depth, and not on the critical depth assumption. This fact is taken into consideration while studying the parabolic broad-crested weir as a discharge measuring device in the present work.

Parabolic broad-crested weir has a cross section of parabolic shape, and a broad-crested in the longitudinal section as shown in Figure (1). The advantages of such weir arise from its simplicity, and accuracy in measuring small and large discharge specially in narrow streams while the discharge is unaffected by submergence up to more than the critical depth.

Parabolic weir can possess greater submergence than rectangular section before the capacity is affected. This is refereed to that, the critical depth for parabolic section is 0.75 H, while it equals 0.67 H for rectangular section. Furthermore the parabolic shape is more sensitive to small heads than rectangular section because Q α H^2 in the former shape, while Q α $H^{1.5}$ in the later one.

The brink or the end depth, is the depth of flow at the end of the weir crest. The brink depth is considered one of the important characteristics since it affects the design of stilling basin below the fall. In addition, it may be used as measuring flow method of drops and waterfalls.

The end depth has been extensively investigated for rectangular channels, and a list of references on this subject has been reported in [14]. Some investigations, to a smaller extent, have been applied for trapezoidal channels [15]. A little work has been done on the end depth for circular channel [16, 17]. In contrast to these, a very little work has been carried out on the brink depth for parabolic, and triangular sections.

Diskin [16] developed equations for the end depth for exponential channels with zero pressure assumption at the end section, giving a theoretical value of the brink depth for parabolic section equals 0.731 of the critical depth. Diskin's work was improved later by Rajaratnam [18], who derived generalized equations for exponential channels for non-zero pressure at the end section. Rajaratnam and Muralidhar [19] presented theoretical, and experimental studies for the depth of exponential channels. The momentum theorem is applied resulting an end depth equation depends on the value of the pressure value at the brink section. Experimentally, the brink depth ratio was found to be 0.772 of the critical depth.

From the above discussion, it is clear that an accurate evaluation for the end depth of parabolic section is not reported. The only given value by Diskin, $y_b = 0.731\ y_c$, is not true because the pressure at the brink section has a certain value and not zero as assumed. The equation predicted by Rajaratnam does not give a definite value for the brink depth, since it depends on the value of the pressure coefficient which is not evaluated as yet either theoretically or experimentally for parabolic section.

The present study is intended to investigate the characteristics of the flow over parabolic broad-crested weir which have not been studied previously. The analysis aimed at predicting an accurate head-discharge relationship. The problem is investigated theoretically by applying the energy equation taking into account the loss of the flow energy. A comprehensive experimental study was conducted including free and submerged weir conditions.

2. THEORETICAL STUDY

2.1 The Depth Of Flow Over The Weir

Experiments showed tat the flow over parabolic weir is characterized by existing a contracted section for all values of L/H from 12 to 2.5. Hence, the depth of flow over the weir is defined as the contracted depth as shown in Figure (1). The depth of flow, y, can be obtained by applying the energy equation at section 1-1, where the head H is measured, and section 2-2 where the contraction of flow occurs. To get an accurate evaluation for the flow depth, the loss of energy h_L between the above two sections should be taken into account.

Equating the specific energy equations at section 1-1, and 2-2 considering the apex line as a datum we get;

$$H_o = y + \frac{\alpha_2 v^2}{2g} + h_L \qquad (1)$$

Substituting for $h_L = \eta \dfrac{v^2}{2g}$, equation (1) becomes;

$$H_o = y + \frac{v^2}{2g}(\alpha_2 + \eta) \qquad (2)$$

where, $H_o = H + \dfrac{\alpha_1 v_a^{\,2}}{2g}$,

η - is the coefficient of head loss,

v_a - is the approaching flow velocity, $v_a = \dfrac{Q}{A_1}$,

A_1 - is the flow cross section area at section 1-1.

Assuming $\alpha_1 = \alpha_2 = 1.0$, and introducing the velocity coefficient C_v to account for the loss of energy, where $C_v = 1/\sqrt{1+\eta}$, in equation (2) yields;

$$H_o = y + \frac{Q^2}{2gA_2^2 C_v^{\,2}} \qquad (3)$$

where, A_2 is the flow cross section are at section 2-2 which is the area of parabola, $A_2 = \frac{2}{3}Ty$, and T is the top width of flow.

The parabola's equation may be written as, $x^2 = 2\ Py$, where P is the parameter of the parabola.

Putting $x = \frac{T}{2}$ in the parabola's equation yields; $T^2 = 8PY$. Hence, $A_2 = \frac{4}{3} y\sqrt{2Py}$, and $A_c = \frac{4}{3} y_c \sqrt{2py_c}$, where A_c and y_c are the cross section area and the depth of critical flow, respectively. The critical depth, y_c for parabolic section may expressed as;

$$\frac{Q^2}{g} = \frac{A_c^3}{T_c} = \frac{64}{27} P y_c^4 \qquad (4)$$

Substituting for $\dfrac{Q^2}{g}$ from (4) in (3) we get;

$$y^4 - H_o y^3 + \frac{y_c^4}{3C_v^2} = 0 \qquad (5)$$

Equation (5) is a quartic equation for y. Using Ferrari's solution [20,21], Eq. (5) has the following four roots;

$$y_1 = \frac{H_o}{2}\left[0.5 + M - [(0.5+M)^2 - 4(K+N)]^{1/2}\right], \qquad (6.a)$$

$$y_2 = \frac{H_o}{2}\left[0.5 + M + [(0.5+M)^2 - 4(K+N)]^{1/2}\right], \quad (6.b)$$

$$y_3 = \frac{H_o}{2}\left[0.5 - M + [(0.5-M)^2 + 4(K-N)]^{1/2}\right], \quad (6.c)$$

$$y_4 = \frac{H_o}{2}\left[0.5 - M - [(0.5-M)^2 + 4(K-N)]^{1/2}\right], \quad (6.d)$$

where;

$$M = (2K + 0.25)^{1/2} \quad (7)$$

$$N = \left[K^2 - \frac{1}{3C_v^2}\left(\frac{y_c}{H_o}\right)^4\right]^{1/2} \quad (8)$$

$$K = -\frac{2}{3C_v}\left(\frac{y_c}{H_o}\right)^2 \operatorname{cosec} 2\alpha, \quad (9)$$

$$\tan\alpha = (\tan\beta_1/2)^{1/3}, \ |\alpha| \le 45°, \quad (10)$$

$$\sin\beta_1 = -\frac{16}{9}\frac{1}{c_v}\left(\frac{y_c}{H_o}\right)^2, \ |\beta| \le 90°, \quad (11)$$

Equation (6.d) gives a negative value for y, while Eqs. (6.a,b, and c) give positive values. In Eq. (6.b) $y_2 > y_c$, while in Eqs (6.a and c) $y_3 < y_1 < y_c$.

Referring to Eq (11), the value of sin β_1 ranges from 0 to $\pm$ 1 with two extreme limits;
0 and $\pm$ 1.

Substituting in Eq. (11) for the above critical limits we get;

(i) For $\sin\beta_1 = 0$, $\beta_1 = 0$ $C_v = \infty$, $y_2 = H_o$, and $y_1 = y_3 = y_4 = 0$.

(ii) For $\sin\beta_1 = \pm 1$, $\beta_1 = \pm\frac{\pi}{2}$, $c_v = \mp\frac{16}{9}\left(\frac{y_c}{H_o}\right)^2$, ,
$y_1 = y_2 = 0.75\,H_o$, $y_3 = 0.25\,H_o$, and
$y_4 = -0.75\,H_o$.

The analysis of the above values of the flow depth, y, indicates that, in the first case the flow is stagnant. In the later case, the depth of flow over the weir has two values; y_1 represents the flow depth in case of free flow, and y_2 is the flow depth in submerged weir condition. The value y_3 rationally speaking can not express the depth of flow over weir, since it ranges from 0 to 0.25 H_o.

Consequently, the depth of flow over weir y_1 and y_2 might be expressed by y_f and y_s referring to free and submerged weir conditions in forms;

$$y_f = \frac{H_o}{2}\left[0.5 + M - [(0.5+M)^2 - 4(K+N)]^{1/2}\right], \text{and} \quad (12)$$

$$y_s = \frac{H_o}{2}\left[0.5 + M + [(0.5+M)^2 - 4(K+N)]^{1/2}\right], \quad (13)$$

2.2 The Velocity Coefficient

The velocity coefficient, C_v, is considered an important parameter for studying the characteristics of flow over the weir, since it expresses the energy lost. Hence, the value of the coefficient C_v strongly affects the values of flow depth and discharge coefficient of weir. It is fruitful to derive a theoretical relationship relates the velocity coefficient C_v, to the ratio y_c/H_o.

Referring to Eq. (11), the values of sin β_1 and C_v are plotted for different values of y_c/H_o and shown in Figure (2). According to Eq. (11) the extreme values for the coefficient C_v may obtained from the following two conditions;

(i) when $\sin\beta_1 = 0$, $C_v = \infty$, and

(ii) when $\sin\beta_1 = -1$, $C_v = \frac{16}{9}\left(\frac{y_c}{H_o}\right)^2$.

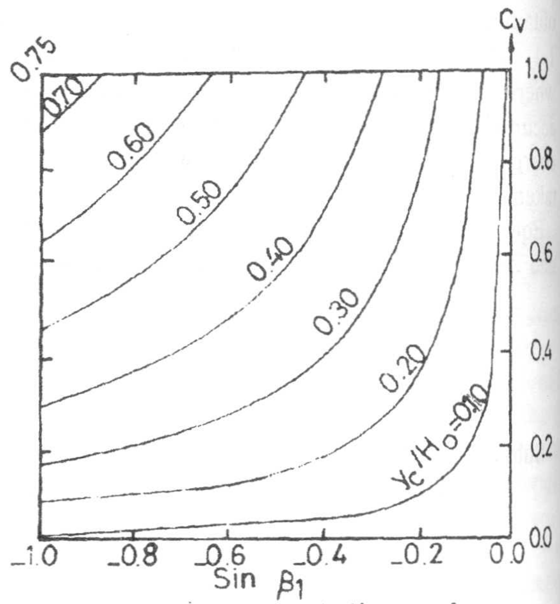

Figure 2. Representation of $\sin\beta_1 = -\frac{16}{9}\left(\frac{y_c}{H_o}\right)^2\frac{1}{C_v}$

However, the coefficient C_v could not possess practical values beyond unity. Hence, the limits of C_v should be ranged from $\frac{16}{9}(\frac{y_c}{H_o})^2$ to 1.0 as depicted in Figure (3) Assuming an average value between the above two limits, the coefficient C_v approximately may obtained as;

$$C_{v_{avg}} = 0.5 + \frac{8}{9}(\frac{y_c}{H_o})^2 \tag{14}$$

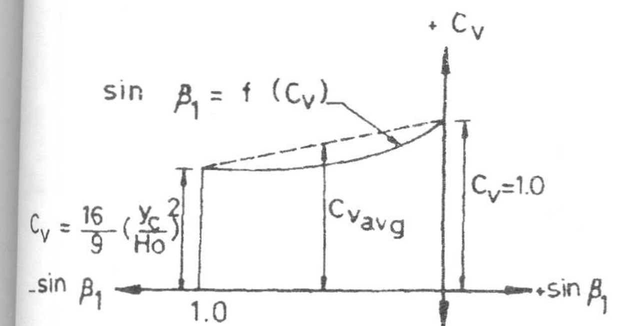

Figure 3. Interpolation of sin β_1 = f (C_V).

Exact expression for C_v may developed by integrating Eq. (11) with respect to C_v from $C_v = \frac{16}{9}(\frac{y_c}{H_o})^2$ to C_v= 1.0 for constant values of $\frac{y_c}{H_o}$ varying from 0 to 0.75.

then,

$$\int_{C_v=\frac{16}{9}(\frac{y_c}{H_o})^2}^{C_v=1.0} [-\frac{16}{9}(\frac{y_c}{H_o})^2 \frac{1}{c_v}]\, dC_v = \frac{16}{9}(\frac{y_c}{H_o})^2 \ln \frac{16}{9}(\frac{y_c}{H_o})^2 \tag{15}$$

Dividing Eq (15) by the difference

$\Delta C_v = 1 - \frac{16}{9}(\frac{y_c}{H_o})^2$, and equating the product to the right hand side of equation (11), we get;

$$C_v = \frac{\frac{16}{9}(\frac{y_c}{H_o})^2 - 1}{\ln \frac{16}{9}(\frac{y_c}{H_o})^2}, \quad 0 < \frac{y_c}{H_o} < 0.75 \tag{16}$$

Equation (16) is applicable when $0 < y_c/H_o < 0.75$. Plotting Eq (16) in Figure (4) indicates that for $y_c/H_o \geq 0.65$, a linear relationship between C_v and y_c/H_o is exist and can be expressed as;

$$C_v = \frac{4}{3}(\frac{y_c}{H_o}), \tag{17}$$

from which $\quad y_c = 0.75\ H_o\ C_v \quad (18)$

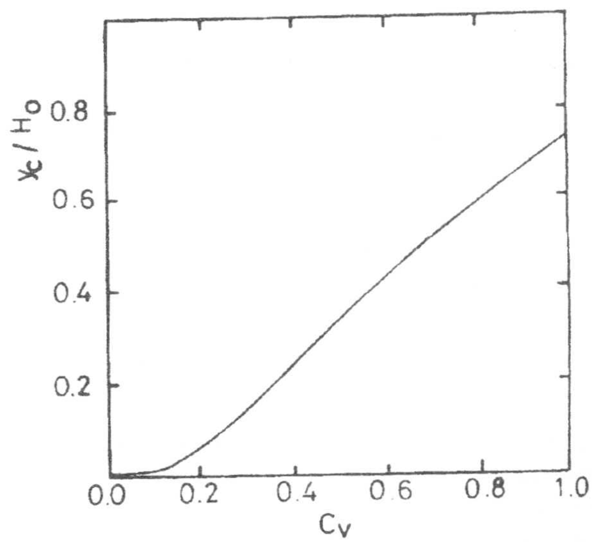

Figure 4. Relation C_V-$\frac{y_c}{H_o}$.

2.3 *The Discharge Coefficient*

Since the discharge coefficient C_d is mainly affected by the energy loss, it may correlate with the coefficient C_v as follows;

As shown in Appendix (1), the discharge equation for parabolic sharp crested weir takes the form;

$$Q = \frac{\pi}{2} C_d \sqrt{gP}\ H_o^2 \tag{19}$$

Referring to Eq (4) we get;

$$y_c^4 = \frac{27}{64} \cdot \frac{Q^2}{gP} \tag{20}$$

Substituting for Q from Eq (19) in Eq (20), yields;

$$C_d = \frac{16}{3\sqrt{3}\,\pi}\left(\frac{y_c}{H_o}\right)^2 \simeq 0.98\left(\frac{y_c}{H_o}\right)^2 \qquad (21)$$

From Eqs. (16) and (21), a general relationship, correlates C_v and C_d may obtained

$$C_v = \frac{\frac{\sqrt{3}}{3}\pi C_d - 1}{\ln \frac{\sqrt{3}}{3}\pi C_d}, \qquad 0 < C_d < \frac{\sqrt{3}}{\pi} \qquad (22)$$

Equations (22) limits the variation of C_d as, $0 < C_d < \frac{\sqrt{3}}{3}$. However, as shown in Figure (5) a simple relationship between C_v and C_d may be developed for values of $C_v \geq 0.85$ by correlating Eqs. (17) and (21) as follows;

$$C_d = \frac{\sqrt{3}}{\pi} C_v^2 \simeq 0.5511\, C_v^2 \qquad (23)$$

It is obvious from eqs. (21), (22) and (23), that C_d is independent on the parabola parameter P.

2.4 *Depth -Discharge Relationship (rating curve relation)*

It is obvious from the above analysis that, the depth of flow over free weir is less than the critical depth. Hence, the discharge equation based on the critical depth seems to be inaccurate. However, the direct measurement of the head on weir H, and the depth over the weir y gives precise evaluation for the discharge over the weir.

A direct relationship between y_f and y_c may obtained for free weir condition by substituting for y_c/H_o with values ranges from 0.65 to 0.75 in Eqs (12) and (16). Then the corresponding values of y_f/H_o are calculated. The governing relationship between y_c/H_o and y_f/H_o in this case may written as;

$$\frac{y_c}{H_o} = 0.92 + 0.427 \ln\left(\frac{y_f}{H_o}\right) \qquad (24)$$

Substituting for y_c from Eq (4) in Eq (24), yields;

$$Q = \left(1.12 + 0.53 \ln \frac{y_f}{H_o}\right)^2 \sqrt{gp}\, H_o^2 \qquad (25)$$

Equation (25) expresses the depth-discharge relationship for values of $0.56 \leq y_c/H_o \leq 0.75$.

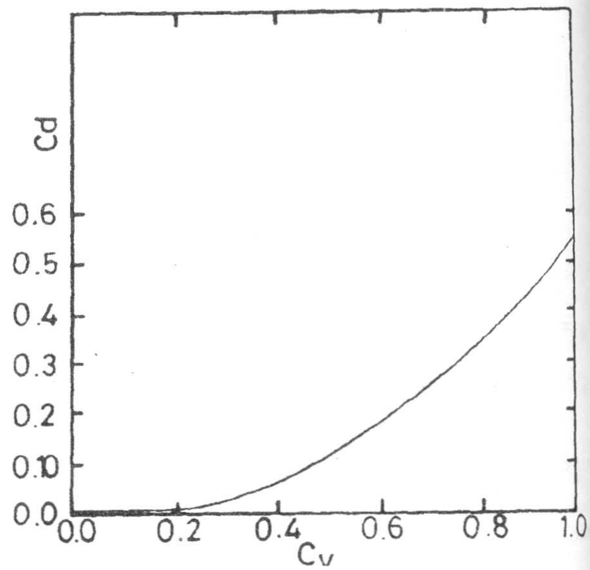

Figure 5. Relation C_v -C_d.

2.5 *Brink Depth*

Diskin and Rajaratnam [16,19] analysed the brink depth ratio, y_b/y_c using the momentum equation. The inaccurate evaluation of the pressure values at the brink section led to the discrepancy between the theoretical (0.731) and experimental (0.772) values of the brink depth ratio.

Evidently, in the previous studies, the energy equation was not employed to theoretically evaluate the brink depth. In this article, the end depth is analysed theoretically using the energy equation as follows.

Equating the specific energy equations at sections 2-2, and 3-3, and neglecting the loss of energy, yields;

$$y_b^4 - y_o\, y_b^3 + \frac{y_c^4}{3} = 0 \qquad (26)$$

Solving Eq (28) using the same procedure applied before for Eq. (5), we get;

$$\sin\beta_2 = -\frac{16}{9}\left(\frac{y_c}{y_o}\right)^2 \tag{27}$$

Substituting for $y_o = 0.75\sqrt{c_v}\,H_o$ in Eq. (29) gives;

$$\sin\beta_2 = -\left(\frac{16}{9}\right)^2\frac{1}{c_v}\left(\frac{y_c}{H_o}\right)^2;$$

from which, for the Case of $\sin\beta_2 = -1$,

$$y_b = \frac{9}{16}\sqrt{c_v}\,H_o \tag{28}$$

Dividing Eq (28) by Eq. (18), we obtain the brink depth ratio in the form

$$\frac{y_b}{y_c} = 0.75\sqrt{\frac{1}{c_v}} \tag{29}$$

3. EXPERIMENTAL STUDY

In the present paper, the experimental study is intended to check the predicted equations for; depth of flow over the weir, y_f and y_s, the coefficients, C_v and C_d, the depth-discharge relationship, and the brink depth, y_b. Experiments were performed also, to investigate the water surface profile and the submergence criterion.

3.1 *Experimental Arrangements*

Experimental work was carried out in the laboratory of Irrigation and Hydraulics research, Faculty of Engineering, Alexandria University.

Experiments were conducted in two horizontal rectangular channels. The first has a 4.0 m length, 0.4 m height, and 0.185 m width. The second has 9.0 m length, 0.5 m height, and 0.395 m width. The channels are fabricated from, 8 mm perespex sheets supported by a steel frame.

Four wooden and coated models for the parabolic broad-crested weir were used in the experiments. The first has crest length, L = 70 cm and parameter, p = 2.5 cm. The other three models having equal length, L = 60 cm, and different parameters; p = 5.0, 7.5, and 10 cm. The first model was inserted in the first channel with apex height, d = 10.4 cm above the channel bottom. The other models were installed in the second channel with height, d = 15.5 cm for each one.

Different discharges were allowed to pass over each weir model covering a range of L/H from 2.5 to 12. For each discharge, the weir head, H, the depth of flow over the weir y, and the brink depth y_b were measured by point gauge. The discharges were measured by a v-notch weir. Submergence by tail water was controlled by adjusting a sliding gate at the end of each channel. All depths were measured with respect to the center line (apex line) of the weir.

3.2 *Experimental Results*

3.2.1 *Flow Surface Profile*

The flow depths were measured longitudinally along the center line of the weir at distances every 2.5 cm. The flow surface profile is plotted with respect to the ratio L/H as shown in Figure (6). In addition to the vertical contraction of flow caused by the weir hump, a lateral contraction accrued due to transition from channel rectangular section to the weir parabolic section. The vertical contraction affects the flow by creating a contracted section located at distance from the entrance increases as the discharge increases. Due to the lateral contraction, cross waves developed with symmetrical formation with respect to the weir center line. For values of $L/H \geq 8$, the intensity of waves increases and the flow behaves similar to the flow in long open channel. As the values of L/H decrease the waves intensity decreases to one wave when $L/H \leq 5.0$. Further increase in the discharge causes gradual withdrawal for the wave towards the weir end, creating parallel flow when $L/H \leq 2.5$. For small values of the parabola parameter, P, parallel flow is expected to occur when $L/H < 2,0$. It can conclude that the best condition for weir operation exists when $L/H \leq 5.0$.

3.2.2. *Submergence flow condition*

Submergence of flow occurs when the head-discharge relationship is affected by the downstream water level. It is important, in practice, to determine the downstream submerged head, h_s^*, at which the discharge starts to be affected. Hence, to determine whether the weir is free or submerged. The criterion which governs this problem can be expressed by using starting ratio, S^*, which is defined as, $S^* = 100 \frac{h_s^*}{H}$, in which h_s^* and H are the head downstream and upstream of the weir, with both related to the crest level.

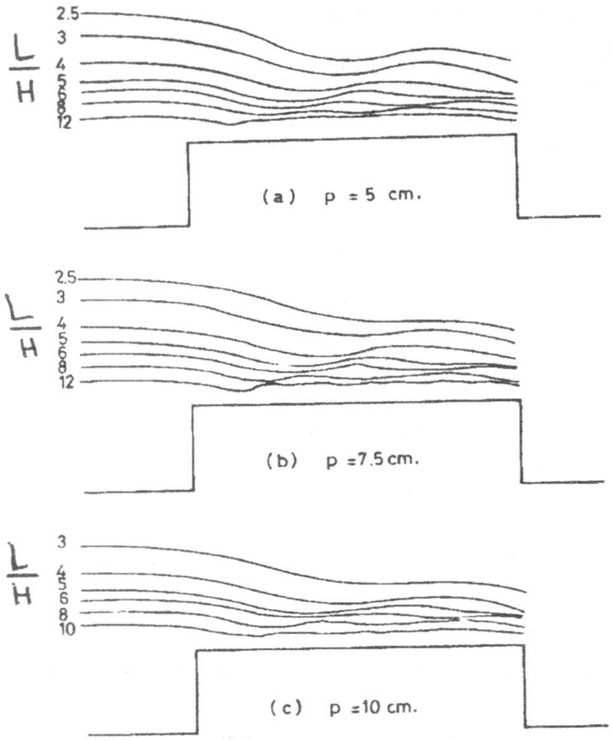

Figure 7. Flow surface profile.

The submergence ratio S^* was investigated experimentally. The downstream water level was gradually raised by adjusting the end gate. The heads h_s and H were measured and recorded at the same time. The head h_s at which the head H begins to increase is considered the depth, h_s^*. The head h_s was measured at section located at point far enough to avoid turbulence downstream the weir, and the effect of backwater created by the end gate. The experimental data are reported in Table (1). In Figure (7), the submergence ratio S^* is plotted versus the ratio H/L. From Figure (7) it can conclude that the average values of S^* is approximately 80% for values of $H/L \leq 0.4$. For values of $H/L > 0.4$ the ratio S^* rapidly falls. Referring to Table (1), its is found that the ratio h_s^*/y_c has an average values equals to 1.15. Consequently submergence criterion is governed by the following relationship;

$$h_s < > 1.15\ y_c$$

If $h_s < 1.15\ y_c$ the weir is free, and if $h_s > 1.15\ y_c$ the weir is considered submerged

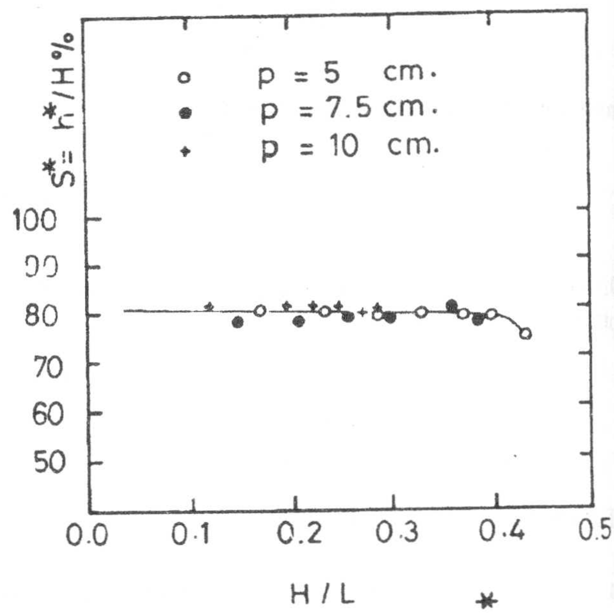

Figure 8. Relation S^* - H/L.

4. RESULTS AND DISCUSSION

Results of more than 100 experimental runs were used to evaluate the accuracy of the developed equations for; the flow depth over the weir y_f or y_s, the velocity coefficient C_v, the discharge coefficient C_d, the depth-discharge relationship, and the brink depth y_b.

4.1. *The Flow Depth Over The Weir*

The total head on the weir, H_o, is calculated using the properties of the approaching flow in rectangular channel section at section 1-1, Figure (1). The values of the critical depth, y_c were calculated according to Eq (4). The values of the velocity coefficient were calculated using Eq (16). Hence, the ratio y_c/H_o and the value of c_v were used to calculated the depth of flow over the weir y_f or y_s corresponds to free or submerged flow conditions, respectively.

Table 1. Experimental data for the submergence ratio S^*, for b = 39.5 and L = 60 cm.

P. Cm.	Q, l/sec.	y_c Cm.	H, Cm	H_s^* Cm	$S^* = \frac{h_s^*}{H}$	h_s^*/y_c
5.0	5.0	6.81	10.13	8.1	0.80	1.19
	10.0	9.63	14.22	11.3	0.795	1.17
	15.0	11.79	17.30	13.55	0.783	1.15
	20.0	13.62	19.90	15.8	0.794	1.16
	25.0	15.23	22.15	17.5	0.79	1.15
	30.0	16.68	24.2	19.1	0.789	1.15
	35.0	18.02	26.04	19.4	0.745	1.08
7.5	5.0	6.15	9.15	7.10	0.775	1.15
	10.0	8.70	12.70	9.9	0.78	1.14
	15.0	10.66	15.57	12.2	0.784	1.14
	20.0	12.31	17.94	14.05	0.783	1.14
	25.0	13.76	19.90	15.8	0.794	1.15
	30.0	15.07	21.66	17.4	0.803	1.16
	35.0	16.28	23.50	18.5	0.787	1.14
10.0	3.74	4.95	7.37	6.0	0.814	1.21
	6.88	6.72	9.92	7.9	0.796	1.17
	9.85	8.04	11.8	9.54	0.808	1.19
	13.37	9.36	13.65	11.05	0.81	1.18
	16.0	10.24	14.9	12.0	0.805	1.17
	19.25	11.24	16.35	13.0	0.795	1.15
	22.44	12.13	17.50	14.10	0.806	1.16

For the free condition, the depth y_f was evaluated according to Eq (12) using the system of Equations, Eq. (7) to Eq (11). The calculated values of y_f were compared to the measuring ones as shown in Table (2). The comparison indicates good agreement with maximum deviation of 5%. However, in most of the cases, the calculated values are higher than the measured ones. This may be referred to the effect of lateral contraction caused by the transition from channel rectangular section to the weir parabolic section. The effect of lateral contraction mainly depends on the flow top width T with respect to the constant width of channel b. Consequently, the calculated and the measured values are getting closer when T increases either by increasing discharges or the parabola parameter P.

As to submerged flow condition, verification of Eq (13) showed good agreement between measured and calculated values of the submerged flow depth, y_s, with deviation does not exceed 6% as shown in Table (3).

4.2. *The Velocity Coefficient, C_v*

The experimental values of the velocity coefficient were obtained by substituting for the measured values of H_o, and y_f in Eq (5) in the form;

$$C_V = \frac{y_c^2}{\sqrt{3}\, y_f^{3/2} \sqrt{H_o - y_f}}$$

The theoretical values of C_v were calculated via applying Eq (16). As shown in Table (2), the experimental, and theoretical values of C_v are in good agreement with maximum relative difference in the range of 3.4%.

The experimental data for free flow condition showed that the ratio y_c/H is always higher than 0.65. Hence, eq (17) is preferable to be used instead of Eq (16) because of its simplicity.

4.3. *The Discharge Coeffient, C_d*

The measured values of Q, and H_o were used in Eq (19) to obtain the experimental values of the coefficient C_d. As reported in Table (2), the theoretical values of C_d obtained by Eq (23) are very close to the experimental ones with maximum deviation of 0.5%.

The experimental values of C_d are plotted against the ratio H/L as shown in Figure (8). It is clear that for the same values of the parabola parameter, P, C_d increases as H/L increases. However some negligible variation of C_d values was found for various values of p for the same value of H/L, e.g., for $H/L = 0.238$ the maximum difference in C_d values was found equals to, $C_d = 0.446$, and 0.45 for $p = 5.0$, and 10 cm, respectively. This difference gives a deviation of 1% with respect to their average values. This result ensures that the coefficient of discharge C_d is independent on the parabola parameter p. The higher values of C_d corresponds to $p = 10$ cm may be related to the effect of the lateral contraction, where the top width T becomes closer to the channel width, b, especially in the models having the same apex height, d. For values of $H/L > 0.2$, the average experimental value of the coefficient C_d was found equal to 0.459, while the theoretical value equals 0.5511 for ideal flow condition ($C_v = 1.0$).

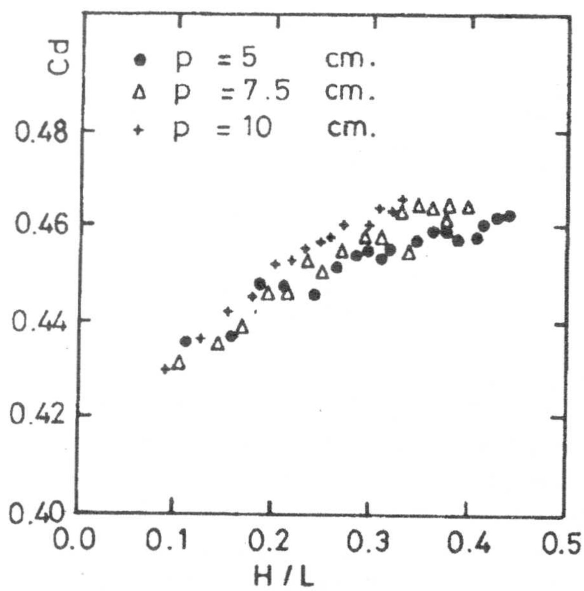

Figure 9. Relation C_d-H/L for various values of p.

4.4. *The depth-Discharge Relationship*

The measured values of H, and y_f were used to calculate the discharge according to Eq (25). The calculated discharges are compared to the measured ones as shown in Figure (9). The comparison shows good agreement with deviation not to exceed 5%.

On the other hand, the average value of the ratio y_c/H was found equals to 0.69 for a range of $L/H \leq$ 5.0. Making use of this value, an empirical equation for the discharge may be written in the form:

$$Q = 0.7335 \sqrt{g\,p}\ H^2, \tag{30}$$

or

$$Q = 2.30 \sqrt{p}\ H^2, \tag{31}$$

where, in eq (31), Q is in m^3/sec. p and H are in meters

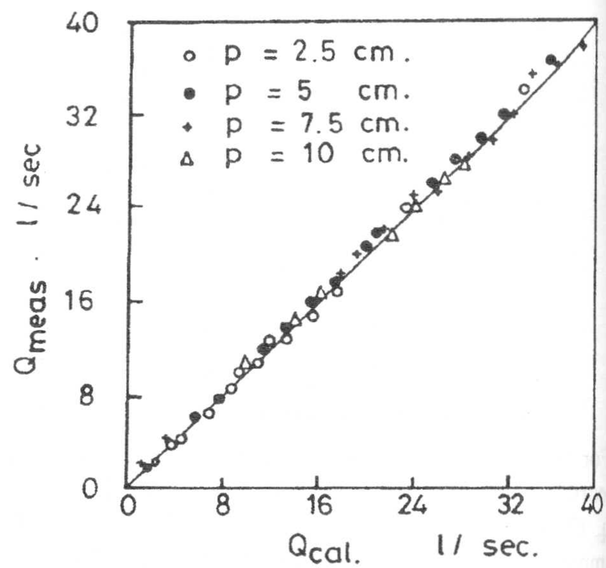

Figure 10. Verification of Eq. (25).

4.5. *The Brink Depth*

As for the brink depth y_b, Eq (29) was checked. The coefficient C_v was computed using Eq. (16). The calculated values of y_b were compared to the measured values. As shown in Table (2), a good agreement exists with a maximum deviation of 6%. On the other hand, the average measured value of the brink depth ratio is found to be 0.773, which is in complete agreement to the value given by Rajaratnam [19].

5. CONCLUSION

An extensive theoretical and experimental studies are presented for the characteristics of the flow over parabolic broad-crested weir. On the basis of these studies it can be concluded that a broad-crested weir of parabolic cross section may be use as a new accurate device to measure stream discharges.

Table 2. Experimental measurements and verification of theoretical Equations of; y_f, C_v, C_d and y_b in case of free flow.

No	Q, ℓ/sec.	H, cm	values of C_v			values of y_f, cm			values of C_d			values of y_b, cm		
			Exp.	Theo. Eq. (16)	% dev.	meas.	Cal., Eq (12)	% dev.	Exp.	Theo., Eq (23)	% dev.	meas.	cal. Eq (29)	% dev.
(1)	(2)	(3)	(4)	(5)	(6)	(7)	(8)	(9)	(10)	(11)	(12)	(13)	(14)	(15)
p= 2.5 cm, d=10.4 cm, L=70 cm, and b=18.5 cm														
1	0.46	3.67	0.898	0.889	-1.0	2.11	2.14	1.4	0.434	0.436	0.5	1.91	1.94	1.6
2	1.13	5.75	0.91	0.894	-1.8	3.30	3.37	2.0	0.44	0.44	0.0	2.95	3.05	3.4
3	2.18	7.9	0.916	0.90	-1.7	4.60	4.7	2.0	0.446	0.446	0.0	4.15	4.22	1.7
4	4.34	11.05	0.913	0.907	-0.6	6.60	6.65	0.8	0.453	0.453	0.0	5.9	5.94	0.7
5	6.35	13.35	0.92	0.907	-1.4	8.25	8.0	-3.0	0.451	0.453	0.4	7.0	7.31	4.4
6	8.71	15.38	0.903	0.917	+1.6	9.70	9.47	-2.40	0.463	0.463	0.0	8.04	8.37	4.1
7	10.98	17.2	0.895	0.919	+2.6	11.05	10.64	-3.7	0.464	0.465	0.1	9.4	9.39	0.0
8	13.12	18.75	0.92	0.92	0.0	12.0	11.62	-3.2	0.465	0.466	0.2	10.2	10.26	0.6
9	15.06	20.0	0.924	0.921	-0.3	12.88	12.48	-3.1	0.466	0.467	0.2	11.0	10.98	0.0
10	16.95	21.17	0.926	0.921	-0.5	13.69	13.23	-3.4	0.467	0.467	0.0	11.35	11.65	2.6
p= 5.0 cm, d=15.5 cm, L=60 cm, and b=39.5 cm														
1	2.09	6.60	0.922	0.891	-3.4	3.70	3.86	4.3	0.436	0.438	0.5	3.45	3.5	1.4
2	4.10	9.22	0.914	0.893	-2.3	5.24	5.41	3.2	0.437	0.439	0.5	4.67	4.89	4.7
3	6.06	11.06	0.937	0.904	-3.3	6.30	6.58	4.4	0.448	0.45	0.5	5.7	5.91	3.7
4	8.09	12.78	0.933	0.903	-3.2	7.32	7.61	4.0	0.448	0.449	0.2	6.62	6.83	3.2
5	10.03	14.25	0.935	0.902	-3.5	8.12	8.49	4.6	0.446	0.448	0.5	7.28	7.62	4.7
6	12.03	15.50	0.94	0.907	-3.5	8.90	9.31	4.6	0.452	0.453	0.2	7.95	8.32	4.7
7	14.02	16.68	0.942	0.909	-3.5	9.62	10.09	4.9	0.455	0.455	0.0	8.54	8.97	5.0
8	16.0	17.80	0.94	0.909	-3.3	10.32	10.77	4.4	0.455	0.455	0.0	9.1	9.58	5.3
9	18.06	18.95	0.935	0.908	-2.8	11.0	11.41	3.7	0.453	0.454	0.2	9.7	10.19	5.1
10	20.18	19.95	0.94	0.911	-3.1	11.60	12.07	4.0	0.456	0.457	0.2	10.25	10.75	4.9
11	21.86	20.72	0.935	0.912	-2.4	12.2	12.57	3.0	0.457	0.458	0.2	10.8	11.18	3.50
12	24.23	21.76	0.942	0.913	-3.0	12.75	13.26	4.0	0.459	0.459	0.0	11.4	11.77	3.2
13	26.26	22.63	0.944	0.914	-3.2	13.25	13.83	4.4	0.459	0.46	0.2	11.9	12.24	2.9
14	28.22	23.50	0.933	0.912	-2.3	13.9	14.28	2.7	0.458	0.458	0.0	12.62	12.7	0.6
15	30.2	24.3	0.935	0.912	-2.40	14.35	14.78	3.0	0.458	0.458	0.0	13.50	13.14	-2.7
16	32.05	24.96	0.931	0.914	-1.8	14.9	15.27	2.5	0.46	0.46	0.0	13.8	13.25	-2.0
17	34.25	25.73	0.938	0.917	-2.3	15.3	15.8	3.3	0.462	0.463	0.2	-	-	-
18	36.55	26.52	0.938	0.919	-2.0	15.85	16.33	3.0	0.463	0.465	0.4	-	-	-
p= 7.5 cm, d=15.5 cm, L=60 cm, and b=39.5 cm														
1	2.06	5.95	0.895	0.886	-1.0	3.41	3.46	1.5	0.431	0.433	0.5	3.10	3.14	1.3
2	4.10	8.35	0.915	0.890	-2.7	4.72	4.89	3.6	0.435	0.437	0.5	4.35	4.43	1.8
3	6.06	10.10	0.924	0.894	-1.4	5.71	5.92	3.7	0.439	0.44	0.2	5.35	5.37	0.4
4	8.14	11.6	0.927	0.902	-2.7	6.67	6.91	3.6	0.446	0.448	0.2	5.88	6.20	5.4
5	10.12	12.94	0.925	0.90	-2.7	7.45	7.70	3.4	0.446	0.446	0.0	6.54	6.92	5.8
6	12.13	14.04	0.934	0.908	-2.8	8.15	8.45	3.7	0.453	0.454	0.2	7.14	7.54	5.6
7	14.13	15.20	0.927	0.906	-2.3	8.84	9.13	3.3	0.450	0.452	0.4	7.69	8.15	6.0
8	16.08	16.11	0.929	0.909	-2.2	9.49	9.76	2.8	0.455	0.455	0.0	8.25	8.68	5.2
9	18.19	17.12	0.925	0.911	-1.5	10.15	10.36	2.0	0.455	0.457	0.4	9.20	9.22	0.2
10	20.04	17.90	0.923	0.913	-2.0	10.60	10.91	2.9	0.458	0.459	0.2	9.85	9.67	-1.8
11	22.00	18.76	0.928	0.912	-1.7	11.15	11.40	2.2	0.457	0.458	0.2	10.7	10.14	-5.2
12	24.74	19.64	0.91	0.907	-0.3	11.85	11.92	0.6	0.453	0.453	0.0	11.15	10.63	-4.7
13	26.10	20.34	0.912	0.911	0.0	12.40	12.41	0.0	0.456	0.457	0.2	11.55	11.05	-4.3
14	28.06	21.00	0.915	0.917	0.2	12.95	12.90	-0.4	0.464	0.463	-0.2	11.84	11.40	-3.7
15	30.17	21.75	0.914	0.919	0.6	13.50	13.40	-0.75	0.464	0.465	0.2	12.30	11.82	-3.9
16	32.05	22.45	0.917	0.917	0.0	13.8	13.81	0.0	0.462	0.463	0.2	12.69	12.2	-3.9
17	33.69	22.93	0.917	0.92	0.3	14.23	14.14	-0.60	0.465	0.466	0.2	13.13	12.49	-4.9
18	36.16	23.75	0.916	0.92	0.4	14.75	14.66	-0.6	0.465	0.466	0.2	13.6	12.94	-4.9
19	38.14	24.50	0.908	0.914	0.7	15.2	15.05	-1.0	0.460	0.46	0.0	14.09	13.33	-5.4

Table 2. Continue

(1)	(2)	(3)	(4)	(5)	(6)	(7)	(8)	(9)	(10)	(11)	(12)	(13)	(14)	(15)
p= 10.0 cm, d=15.5 cm, L=60 cm, and b=39.5 cm														
1	2.02	5.48	0.884	0.888	0.5	3.2	3.19	-0.3	0.432	0.434	0.5	2.83	2.90	2.5
2	4.04	7.70	0.919	0.893	-2.8	4.36	4.52	3.7	0.437	0.439	0.5	3.95	4.09	3.5
3	6.06	9.35	0.925	0.893	-2.8	5.34	5.54	3.75	0.443	0.445	0.5	4.85	4.98	2.7
4	8.09	10.76	0.926	0.902	-2.6	6.2	6.41	3.4	0.446	0.448	0.5	5.45	5.75	5.5
5	10.12	11.96	0.933	0.907	-2.8	6.92	7.19	3.9	0.452	0.453	0.2	6.07	6.42	5.8
6	12.03	13.0	0.93	0.908	-2.4	7.60	7.83	3.0	0.453	0.454	0.2	6.61	6.99	5.7
7	14.13	14.04	0.928	0.911	-1.8	8.30	8.51	2.50	0.456	0.457	0.2	7.13	7.56	6.0
8	16.08	14.94	0.927	0.912	-1.6	8.90	9.07	1.9	0.457	0.458	0.2	7.65	8.07	5.5
9	18.06	15.80	0.924	0.913	-1.2	9.48	9.63	1.6	0.458	0.459	0.2	8.33	8.54	2.5
10	20.04	16.57	0.93	0.917	-1.4	9.96	10.16	2.0	0.462	0.463	0.2	8.84	8.98	1.6
11	22.0	17.44	0.916	0.912	-0.4	10.55	10.61	0.6	0.457	0.458	0.2	9.55	9.43	-1.3
12	23.98	18.12	0.916	0.916	0.0	11.10	11.11	0.0	0.461	0.462	0.2	10.03	9.83	-2.0
13	26.03	18.8	0.919	0.918	-0.1	11.57	11.58	0.0	0.464	0.464	0.0	10.5	10.22	-2.7
14	28.06	19.50	0.914	0.919	0.50	12.12	12.02	-0.8	0.464	0.465	0.2	10.81	10.61	-1.9
15	30.27	20.2	0.916	0.92	0.40	12.60	12.51	-0.7	0.460	0.466	0.0	11.05	11.02	-0.3

As a result of the above theoretical study a group of simple experimentally verified relationships were developed, and could be employed in the following:

1- Estimation of the flow depth over the weir in free, and submerged flow condition: Eqs. (12), and (13).
2. Determination of the velocity coefficient in terms of the critical depth related to the total head on weir; Eqs (16), and (17).
3. Determination of the discharge coefficient with respect to the velocity coefficient; Eqs (22) and (23).
4. Prediction of the weir discharge as function of the head on the weir H, and the depth of free flow over weir y_f; Eq. (25)
5. Evaluation of the brink depth with respect to the critical depth; Eq (29).

According to the experimental study, we can conclude the following:

1. The best condition for the weir operation exists when $L/H \leq 5.0$.
2. The weir can be operated without any effect by tail water on the discharge up to submergence ratio equals 80%, while $H/L \leq 0.4$. The weir is considered free if $h_s/y_c \leq 1.15$.
3. The discharge coefficient is independent on the parabola parameter, and has an average value of 0.459 for $L/H \leq 5.0$.
4. The measured brink depth ratio has an average value of 0.773 of the critical depth.

Finally, Equation (31) is recommended to be practically applied for measuring discharges over broad-crested weir since, one only measuring parameter is needed, which is the head on the weir H.

REFERENCES

[1] A.J.M. Harrison, "The Streamlined Broad-Crested Weir", *proc. of the Institute of Civil Engineers*, London, England, pp. 7028, December, 1967.

[2] R.L. Parshall, "The Improved Venturi Flume". Transactions, *ASCE*, vol. 89, 1926.

[3] G.V. Skogerboe and M.L. HyaH, "Rectangular Cutthroat Flow measuring Flumes"., J. of the Irrigation and Drainage Div., *ASCE*, vol. 93, No. IR 4, pp 1-13, December, 1967.

[4] C.D. Smith, "Open Channel water Measurement With Broad-Crested Weir" *Annual Bulletin of the International Commission on Irrigation and Drainage*, New Delhi, India, 1958.

[5] P. Ackers, W.R. White, J.A. Perkins, and A.J.M. Harrison, *Weirs and Flumes for Flow measurement*, John Wiley and sons New York, N.Y., 1978.

[6] C.D. Smith, and W.S. Liang, "Triangular Broad-Crested Weir" J. of the Irrigation and Drainage Div., *ASCE*, vol. 95, IR 4, pp. 493-502, December, 1969.

[7] Wubbo Boiten and Remmet, H. Pitlo. "The-Shaped Broad-Crested Weir" J. of the Irrigation and Drainage Div, *ASCE*, vol. 108, No. IR2, pp. 142-160, June, 1982.

Table 3. Verification of Eq. (13) for calculating the flow depth, y_s in submerged flow condition.

No.	Q, ℓ/sec	H, Cm	values of y_s, cm		
			meas.	cal., Eq(13)	% dev.
p= 2.5 cm, d=10.4 cm, L=70 cm, and b=18.5 cm					
1	1.13	6.50	5.68	5.97	5.10
2	2.18	8.20	6.91	7.29	5.5
3	4.34	12.73	11.10	11.72	5.6
4	6.57	15.0	13.09	13.67	4.4
5	8.71	17.25	14.98	15.77	5.3
6	10.98	19.65	17.35	18.07	4.2
7	13.12	21.15	18.55	19.42	4.7
p= 5.0 cm, d=15.5 cm, L=60 cm, and b=39.5 cm					
1	2.09	7.54	6.62	6.94	4.8
2	5.00	11.64	10.19	10.7	5.0
3	6.06	12.9	11.25	11.91	5.9
4	8.09	14.22	12.21	12.94	6.0
5	10.03	16.24	14.47	14.93	3.2
6	12.03	17.25	14.86	15.69	5.6
7	14.02	19.9	17.8	18.45	3.7
8	15.96	20.74	18.3	19.10	4.4
9	18.06	22.9	20.8	21.31	2.5
10	20.18	23.38	20.70	21.59	4.3
11	21.86	24.35	21.56	22.51	4.4
12	24.26	25.1	21.96	23.07	5.0
13	26.26	27.9	26.0	26.03	0.0
14	28.22	28.60	26.30	26.66	1.4
p= 7.5 cm, d=15.5 cm, L=60 cm, and b=39.5 cm					
1	2.01	6.2	5.27	5.57	5.7
2	4.04	9.63	8.52	8.89	4.3
3	5.05	10.60	9.4	9.78	4.0
4	8.0	13.64	12.24	12.63	3.2
5	9.76	14.60	12.70	13.43	5.75
6	12.13	15.65	13.50	14.24	5.5
7	14.02	18.0	16.30	16.7	2.5
8	16.32	18.85	16.75	17.37	3.7
9	18.06	20.80	19.2	19.37	0.9
10	20.04	24.45	19.75	19.93	0.9
11	22.06	22.15	20.4	20.52	0.6
12	24.38	22.9	20.8	21.11	1.5
13	26.10	23.86	21.95	22.04	0.4
14	28.06	24.4	22.45	22.47	0.0
p= 10.0 cm, d=15.5 cm, L=60 cm, and b=39.5 cm					
1	2.02	6.60	6.06	6.15	1.5
2	4.10	8.92	7.9	8.23	4.2
3	6.12	10.12	8.60	9.11	5.9
4	8.25	12.30	10.66	11.28	5.8
5	10.12	13.30	11.45	12.10	5.7
6	12.23	15.2	13.74	13.96	3.1
7	14.24	16.0	14.06	14.66	4.3
8	15.96	17.12	15.21	15.74	3.5
9	18.19	18.40	16.45	16.96	3.1
10	20.18	19.11	17.0	17.55	3.2
11	22.44	19.75	17.50	18.03	3.0

[8] H. Rouse, *Fluid Mechanics For Hydraulic Engineers*, McGraw-Hill Book Company, New York, 1938, pp. 319-321.

[9] J.R.D. Francis, and P. Minton, *Civil Engineering Hydraulics*, London, 1986, pp. 285-287.

[10] R.H. French, Open Channel Hydraulic, *McGraw-Hil Book Company*, New York, Toronto, 1986, pp. 336-342.

[11] F.M. Henderson, *Open Channel Flow*, The Macmillan Company, New York, London, 1970, pp. 210-213.

[12] A.J. Clemmens, M.G. Bos, and J.A. Replole. "Contraction Ratios For Weir And Flume Designes" J. of the Irrigation and Drainage Div., *ASCE*, vol. 113, No. 3, pp. 420-424 August 1987.

[13] H.A. Doering sfeld, C.L. Barker, "Pressure-Momentum theory applied to the Broad-Crested Weir" *Transaction of the ASCE*, vol. 106, paper No. 2177, pp. 943-969, 1941.

[14] M.A. Abourehim, "Depths of Flow Over Rectangular Broad-Crested Weir", *Alex. Eng. J.* vol. 30, No. 2, pp. C 55- C 62, April, 1991.

[15] J.K. Robert, and S.F. Soon, "Flow Measurement With Trapezoidal Free overfall" J. of the Irrigation and Drainage Division *ASCE*, vol. 115, No 1, pp. 125-137, February, 1989.

[16] M.H. Diskin, "End Depth At A Drop In Trapezoidal Channels", J. of Hy. Div., *ASCE*, vol. 87, No. Hy. 4, pp. 11-32, July, 1961.

[17] C.D. Smith, "Brink Depth For Circular Channel", J. of Hy. Div, *ASCE*, vol. 88, No Hy 6, pp. 125-134, November, 1962.

[18] N. Rajaratnam, Discussion of "The End Depth at a Drop in Trapezoidal Channels" by M.H. Diskin, J. of the Hy. Div, *ASCE*, vol, 88, No Hy 1, proc. paper 3044, pp. 119-130, January, 1962.

[19] N. Rajartnam, and D. Nuralidhar, "End Depth For Exponential Channels" J. of the Irrigation and Drainage Div, *ASCE*, vol. 90, No IR 1, pp. 17-39, March, 1964.

[20] A.G. Tsypkin, and G.G. Tsypkin, *Mathematical Formallas; algebra, geometry, and mathematical analysis*, Mir publishers, Moscow, 1988.

[21] G.A. Korn, and T.M. Korn, *Mathematical Handbook for Scientist and Engineers*, McGraw-Hill Book Company, New York, London

[22] B.B. Necrasof, *Reference Book in Hydraulics*, Higher Schook, Minsk, 1985, pp. 173.

Appendix 1

Discharge Coefficient for sharp crested parabolic weir[1]

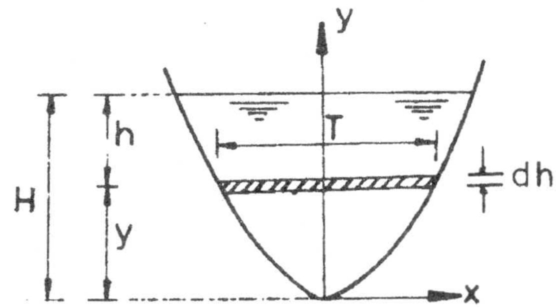

Figure 10. Parabolic sharp crested weir.

Considering a strip of flow with width T, and thickness dh lies at a depth h from the flow surface as shown in Figure (10).

The elementary area of strip $dA = T.dh$, and the theoretical velocity, $v = \sqrt{2gh}$. Hence,

$$Q = \int_0^H C_d T \sqrt{2gh}\, dh . \tag{1}$$

From the equation of parabolu, $T^2 = 8\,py$, where $y = H\text{-}h$, then

$$T = 2\sqrt{2p\,(H-h)} . \tag{2}$$

Substituting for T in Equation (1), yields;

$$Q = 4\, C_d \sqrt{gp} \int_0^H \sqrt{h(H-h)}\, dh . \tag{3}$$

[1] Derivation steps are explicitly given to prove the inaccurate equation (11.9) listed in Reference [22], p. 173.

Equation (3) can be written in the form:

$$Q = 4\,C_d\,\sqrt{gp}\int_{o}^{H}\sqrt{\frac{H^2}{4}-(h-\frac{H}{2})^2}\;dh. \qquad (4)$$

In Equation (4) put $h - \frac{H}{2} = \frac{H}{2}\sin\theta$ and differentiate yields,

$$dh = \frac{H}{2}\text{Cos}\theta\, d\theta,$$

for $h = H$, $\quad \frac{H}{2}\sin\theta = \frac{H}{2}$ and $\theta = \frac{\pi}{2}$,

for $h = 0$, $\quad \sin\theta = -1$ and $\theta = -\frac{\pi}{2}$.

Substituting for the above values in (4), we get;

$$Q=4C_d\,\sqrt{gp}\int_{-\frac{\pi}{2}}^{+\frac{\pi}{2}}\sqrt{\frac{H^2}{4}-\frac{H^2}{4}\sin\theta}\,.\;\frac{H}{2}\cos\theta\, d\theta, \quad (5)$$

from which

$$Q = 4\,C_d\,\sqrt{gp}\,\frac{H^2}{4}\int_{-\frac{\pi}{2}}^{+\frac{\pi}{2}}\text{Cos}^2\theta\, d\theta, \qquad (6)$$

and $Q = 8\,C_d\,\sqrt{gp}\,.\frac{H^2}{4}\int_{0}^{\pi/2}\frac{1}{2}\,(1 + \text{Cos}\,2\,\theta)\,d\theta,$ (7)

then$Q = 8\,C_d\,\sqrt{gp}\,.\frac{H^2}{4}\,\frac{1}{2}\,\left[\theta+\frac{1}{2}\sin 2\theta\right]_{o}^{\pi/2},$ (8)

and finally $\qquad Q = \frac{\pi}{2}C_d\sqrt{gp}\,H^2.$ $\qquad$ (9)